TOTAL REACTION CROSS SECTIONS IN DEUTERON AND PROTON INDUCED REACTIONS

M. Cabibbo and C. Volant

DAPNIA/SPhN, CEA/Saclay, F-91191 Gif-sur-Yvette CEDEX, FRANCE.

(June 28, 2000)

Abstract

Total reaction cross sections for deuteron and proton induced reactions are parameterised through models whose parameters are adjusted to the existing data from low energies to the domain of around GeV per nucleon.

I. INTRODUCTION

The total reaction cross section is one of the first basic measurements needed to understand the nuclear interactions in ion-ion collisions. Its parameterisation is also of great interest and many attempts have been already done [1–8]. Studies of the spallation residue production by means of the reverse kinematics using heavy ions of energies around 1 GeV/nucleon bombarding hydrogen targets (hydrogen and deuterium) are currently performed at GSI Darmstadt (Germany) [9]. The target used is relatively thick and secondary reactions are quite probable. One way to correct the data for them is to rely on reaction cross section parameterisations. This has been done for proton targets but for deuteron targets such work had to be performed. That is the aim of the present report. To be complete we will also applied this formulation to proton induced reactions.

II. USED FORMULATION

We performed a simple routine which permits to calculate the total reaction cross section of deuteron and proton-induced reactions on heavy nuclei. It is based on two models:

For energies per nucleon greater than 100 MeV we use the Karol microscopic model [1]. In this model the reaction probability is calculated assuming the interaction due to single nucleon-nucleon collisions in the region of the overlap between projectile and target. Therefore in this model the choice of the density distribution function plays a crucial rule. In the case of light nuclei (deuteron or proton in our case) coherently with the Karol description this function is assumed as a Gaussian:

$$\rho(r) = \frac{A}{(a\sqrt{\pi})^3} \exp(-(\frac{r}{a})^2) \tag{1}$$

where a is related to the root mean square radius by

$$a = (r.m.s.\ \ radius) * 1.5^{-1/2} \tag{2}$$

In litterature one can find as r.m.s. charge radius of deuteron 2.1 fm [10], but in our routine we fix this value equal 2.8 fm to have a better reproduction of experimental data [2,11]. This last number which corresponds to twice the Compton wave length of the pion is used as the square potential well radius in the simplest model for the deuteron system [12].

In the case of p-induced reaction we fix the correspondent r.m.s. proton radius equal to 1.034 fm. In fact also one can find in litterature [10,13] a r.m.s. proton radius equal to 0.8 fm, but to have a better reproduction of experimental data (see the next section) we choose 1.034 fm which is the radius of equivalent uniform model [13].

For heavier nuclei (A $>$ 40 target nuclei) the density distribution function is obtained in Karol model using the so-called "surface-normalized" Gaussian density distribution. Without going into details a Gaussian form is used

$$\rho(r) = \rho(0) \exp(-(\frac{r}{a})^2) \tag{3}$$

where both $\rho(0)$ and a are parameterised following Karol to fit the Gaussian distribution to the surface of a Fermi distribution. This method permits an analytical solution for the reaction cross section.

Another fundamental ingredient of this model is the average nucleon-nucleon collision cross section $< \sigma >$ which is a function of the incident energy per nucleon (see ref. [1]). This cross section is a weighted average over the proton and neutron numbers of the target and the projectile, between the neutron-neutron (proton-proton) total cross section σ_{ii} and the neutron-proton total cross section σ_{ij}. The parameterisation which we use to take into account the energy dependence of these cross sections is a compromise between a faithful reproduction of the existent experimental data and simple analytical forms which allow fast reconstruction of the cross sections (see ref. [14]).

At low incident energies the Karol model is no more valid because it neglects many typical low energy effects (Pauli blocking, Fermi motion, Coulomb barrier). Therefore for energies lower than 100 MeV per nucleon, the total reaction cross section is calculated, in our routine, using the Kox et al. geometrical formula [3]. This semiempirical approach starts from a simple geometrical formula corrected by the Coulomb barrier B_C

$$\sigma_R = \pi {R_{int}}^2 [1 - \frac{B_C}{E_{cm}}] \qquad\qquad B_C = \frac{Z_p Z_t e^2}{r_c (A_p^{1/3} + A_t^{1/3})} \tag{4}$$

where σ_R is the total reaction cross section, $A_{p(t)}$ and $Z_{p(t)}$ are, respectively, the mass and proton number of projectile (target), and E_{cm} is the kinetic energy in the centre of masse.

Kox et al. propose to divide the interaction radius R_{int} into a volume term $R_v = r_0(A_p^{1/3} + A_t^{1/3}) = R_p + R_t$ and in a surface term R_s:

$$R_{int} = R_v + R_s \tag{5}$$

Introducing this surface term, it is possible to include in a simple geometrical description those part of the total reaction cross section due to the interaction between the projectile and the target in the region of the overlap. In Kox formula the surface term is given by:

$$R_s = r_0 [a \frac{A_p^{1/3} A_t^{1/3}}{A_p^{1/3} + A_t^{1/3}} - c_k] + D \tag{6}$$

The first term takes into account the mass asymmetry and is related to the volume overlap between projectile and target, c_k is an energy dependent parameter which takes care of increasing surface transparency as the projectile energy increases. These two terms represent the main physical effects introduced by R_s.

The last term is the neutron excess term D

$$D = \frac{5(A_t - 2Z_t)Z_p}{A_p A_t} \tag{7}$$

It takes into account the fact that at low incident energy the total cross section for neutron-proton (n-p) collisions is greater than those for n-n and p-p collisions. Therefore this term is very important for heaviest or neutron-rich targets specially in the case of proton projectile.

Our routine uses an adjusted Kox formula. In the case of deuteron the projectile volume radius R_p is fixed (in $R_v = R_p + R_t$ and in B_C) to be equal to 1.9 fm. Remark that a r.m.s. value of 1.95 fm for deuteron is also quoted in ref. [15]. With this choice, which permits a general agreement with the experimental data (see next section), we take into account the loose structure of the deuteron. In this way we will have for R_v and B_C

$$R_v = r_0 A_t^{1/3} + 1.9 \qquad\qquad B_C = \frac{Z_p Z_t e^2}{(r_c A_t^{1/3} + 1.9)} \tag{8}$$

where r_0 was fix equal to 1.1 fm as in standard Kox parameterisation. For r_c we use values between r_c=1.1 and r_c=1.3 fm (see the pictures in sec.III); the last one being the value used in standard Kox parameterisation.

Remark we do not modify the asymmetry term in eq.(II.6) which could be felt as an inconsistency because we change R_p for deuteron from $1.1 * 2^{1/3} = 1.39$ to 1.9 fm. In fact from a microscopical point of view the interaction probability in the overlap region depends not only upon the overlap volume but also from the density in this region. In deuteron case there is an increase of the overlap volume due to its large diffusivity but on the other hand the external projectile density is lower. In the parameterisation of Kox et al. the density profile is not taken into account. So the mentioned effect cannot be included on the asymmetry term without including new unknown parameters.

In the case of p-induced reaction calculations we fix R_p=1.fm (in $R_v = R_p + R_t$ and in B_C) and r_c=r_0=1.1 fm.

In our routine the transparency terms of R_s (c_k in eq. (II.6)) depends on the incident energy per nucleon in the following way:

$$c_k = 2.2704 * log_{10}(E_n) - 2.6173 \tag{9}$$

This behavior was obtained by fitting the c_k-values obtained by Kox et al. for lower energies [3].

III. COMPARISON TO EXPERIMENTAL DATA

A. Deuterons

We present some comparisons between results from our routine and experimental data. We calculate (see fig.1-4) the total reaction cross section of $d + Pb, Zr, Ni, Ca$ collisions; using the parameterisation explained in the previous section. In particular for each reaction we show the calculation of σ_R using both mentioned values for the r_c parameter (1.1 and 1.3 fm for incident energy lower than 100 MeV/nucleon).

One can see a general agreement with experimental data; the small discontinuity at 100 MeV per nucleon is due to the change of formula. For the lowest energies it is difficult to say which value for the r_c parameter gives better results. One can note that using the standard value r_c=1.3 fm we have a better agrement for the two heaviest target nuclei (Pb and Zr), but at the same time we have a worst continuity at 100 MeV with respect to r_c=1.1 fm. In general at low energy the choice of r_c=1.3 fm could be preferred because these results are obtained by changing in the Kox parameterisation only one parameter: the projectile volume radius R_p.

For the highest energies, in fig.1 and 3a) results obtained with two different values of deuteron r.m.s. radius: 2.8 and 2.1 fm are shown to illustrate the sensitivity of Karol formula on this parameter. The good general agreement obtained fixing this parameter equal to 2.8 fm is very encouraging. Considering the scarse data available at the highest bombarding energies, this justifies our choice for this parameter in Karol formula.

B. Protons

In fig.5 is shown a comparison of our calculation with experimental data [16] in the case of $p + {}^{207.2}Pb$ reaction. As can be seen in this case we obtain a very good continuity at 100 MeV using the present parameterisation. The agreement with the data is also quite satisfactory specially in the high energy regime. Note that we adapted Kox parameters to have a good continuity with the Karol calculations. See also on the figure the low energy calculation using the standard Kox parameter (r_c=1.3 instead of r_0=1.1 fm).

In fig.6 is shown a standard Kox calculation for the full energy range. Note the discontinuity at 200 MeV because above this energy the neutron excess term D is put equal to zero. The authors of ref. [3] recommand to do so above 200 MeV/nucleon because σ_{nn} and σ_{pp} are no more so different from σ_{np}. This however is not completely true (see next section and fig.10). In principle to solve this problem, an energy dependence of the D term should be considered. This is yet out of the scope of this report.

C. Comparison with other formulations

In litterature different semiempirical models are available; see for example Tripathi et al. [4,5] and Prael and Chadwick [6] which tend to be universal.

To be complete we show also the results obtained using other existing semiempirical models in their published standard versions. In fig.7 the standard Tripathi et al. model [4,5] and the Wellisch [6,7] formulation is applied to the $p + {}^{207.2}Pb$ reaction. As can be seen for the lowest energies the corrected Wellisch [6,7] formulation reproduces the experimental

data better than our adjusted Kox formula. However our parameterisation works more nicely at the highest energies. The published Tripathi et al. parameterisation [4,5] gives worst results but the nice agreement shown in ref. [8] with the same model has to be clarified. In fig.8 and fig.9 are shown the standard Tripathi calculations for the reactions $d + Pb$ and $d + Ni$ respectively. The two curves (full and dashed) in each picture are obtained using two different values of the deuteron r.m.s. radius (2.8 and 2.1 fm respectively). For the targets, the r.m.s. radii are taken from [10] as recommanded in [4,5]. The agreement with the experimental data is worst than the one obtained in the present work. One can also notice the weaker sensitivity of the Tripathi et al. calculations comparative to our formulation (see fig.1 and 3a) on this parameter.

IV. ENERGY DEPENDENCE OF σ_R

Fig.10 shows the p-p and n-p total reaction cross section as function of the bombarding energy calculated with the parameterisation of J. Cugnon et al. [14] used here. Clearly the maximum transparency (minimum in σ_R) seen around 300 MeV/nucleon in fig. (1-9) arises from the variation of the nucleon-nucleon cross section as already pointed out in ref. [2]. Above this minimum σ_R starts again to increase because of the opening of the pion production.

Note a discontinuity at 80 MeV due to the change of parameterisation formula at this energy in [14]. In the present work only energy above 100 MeV are considered. Also, in intranuclear calculations these low energy collisions are of low importance.

V. CONCLUSION

The present parameterisation can permit to perform the needed corrections mentioned in the introduction. The discrepancy observed at low energy between our parameterisation and experimental data (see fig.1) is reasonable because in our formulation we don't take into account different physics effects releated to: projectile wave length, energy dependence of Coulomb barrier, overlap volume (for deuteron case), energy dependence of D term. On the other hand the good agreement for the high energy range is very encouraging since that is mainly in that region that the cross-section evaluation are needed. The main ingredient is the deuteron r.m.s. radius which has been adjusted to the data but the obtained phenomenological value can be reasonably well justified on a theoretical ground. Data above 400 MeV/nucleon for deuteron total reaction cross section are not available for targets heavier than carbon [18]. This makes difficult a complete check of the present predictions.

REFERENCES

[1] Paul J. Karol, Phys. Rev. C 11 (1975) 1203 .

[2] R. M. DeVries and J. C. Peng, Phys. Rev. C 22 (1980) 1055.

[3] S. Kox et al., Phys. Rev. C 35 (1977) 1678.

[4] R. K. Tripathi, F. A. Cucinotta, J. W. Wilson, Nucl. Instr. and Meth. B 117 (1996) 347-349.

[5] R. K. Tripathi, F. A. Cucinotta, J. W. Wilson, "Universal Parameterization of Absorption Cross Sections" NASA Technical Paper 3621 (January 1997).

[6] R. E. Prael and M. B. Chadwick, "Applications of Evaluated Nuclear Data in LAHET^{TM} Code", Proceedings of the International Conference on Nuclear Data for Science and Technology, May 19-24, 1997 Trieste, Italy (1997).

[7] H. P. Wellisch and D. Axen, Phys. Rev. C 54 (1996) 1329.

[8] R. E. Prael et al., "Plots Supplemental to: Comparison of Nucleon Cross Section Parameterization Methods for Medium and high Energies", Los Alamos National Laboratory report LA-UR-98-5843 (December 1998).

http://www-xdiv.lanl.gov/XCI/PEOPLE/rep/plist.htlm

[9] W. Wlazło et al., Phys. Rev. Lett. 84 (2000) 5736 .

F. Rejmund et al., submitted to Nucl. Phys. A.

J. Benlliure et al., submitted to Nucl. Phys. A.

T. Enqvist et al., submitted to Nucl. Phys. A.

[10] H. de Vries, C.W. de Jager and C. de Vries, Atom. Data and Nucl. Data Tables 36, 495-536 (1987).

[11] Nguyen Van Sen et al., Phys. Lett. 156B (1985) 187.

[12] E. Segre, Nuclei and particles, W. A. Benjamin, Inc. New York 1965 Amsterdam.

[13] H. R. Collard, L. R. B. Elton, and R. Hofstadter, in *NuclearRadii*, edited by H. Schopper (Springer-Verlag, Berlin, 1967), Landolt-Bornstein, New Series, Vol.2.

[14] J. Cugnon, D. L'Hôte, J. Vandermeulen, Nucl. Instr. and Meth. B 111 (1996) 215.

[15] J. Arvieux and J. M. Cameron Adv. in Nucl. Phys., Vol. 18. Edited by J. W. Negele and Erich Vogt (Plenum Publishing corporation, 1987).

[16] B.C. Barashenkov, Cross sections of Interactions of Particle and Nuclei with Nuclei, JINR, Dubna, 1993.

[17] A. Auce et al., Phys. Rev. C 53 (1996) 2921.

[18] J.Jaros et al., Phys. Rev. C 18 (1978) 2273.

FIGURES

FIG. 1. (a)Total reaction cross sections in mb as function of incident energy per nucleon for the system $d + ^{208}Pb$. The full line is our adjusted Kox-Karol calculation using r_c=1.3 fm for $E/n < 100$ MeV (see text), the experimental data (open symbols) are from ref. [2,17]. (b) The same of (a) but using r_c=1.1 fm. The dashed line in (a) is a Karol calculation obtained using a r.m.s. deuteron radius equal 2.1 instead of 2.8 fm (full line).

FIG. 2. (a)Total reaction cross sections in mb as function of incident energy per nucleon for the system $d+^{90}Zr$. The full line is our adjusted Kox-Karol calculation using r_c=1.3 fm for $E/n < 100$ MeV (see text), the experimental data (open symbols) are from ref. [2,17]. (b) The same of (a) but using r_c=1.1 fm.

FIG. 3. The same as in fig.1 but for the system $d + ^{58}Ni$. In this case the experimental data (open symbols) are taken from ref. [11,17].

FIG. 4. The same as in fig.2 but for the system $d + ^{40}Ca$. In this case the experimental data (open symbols) are taken from ref. [2,11,17].

FIG. 5. Total reaction cross sections in mb as function of incident energy for the system $p + ^{207.2}Pb$. The dashed line is a standard Kox calculation. The full line is our calculation using the parameterisation presented in section II. The experimental data (open symbols) are from ref. [16].

FIG. 6. The same as in Fig.5 but only with a standard Kox calculation for the full energy (full line). The experimental data (open symbols) are from ref. [16].

FIG. 7. Total reaction cross sections in mb as function of incident energy for the system $p + ^{207.2}Pb$. The full line corresponds to the formulation of Prael and Chadwick and the dashed line is a Tripathi et al. calculation (see text). The experimental data (open symbols) are from ref. [16].

FIG. 8. Tripathi et al. calculations for the total reaction cross section (mb) for the reaction $d + ^{208}Pb$. The two calculations was obtained using a r.m.s. deuteron radius equal 2.8 fm. (full line) and 2.1 fm. (dashed line). The experimental data (open symbols) are from ref. [2,17]

FIG. 9. The same of fig.8 but for the system $d + ^{58}Ni$. In this case the experimental data (open symbols) are taken from ref. [11,17].

FIG. 10. Proton-proton and neutron-proton total reaction cross sections as function of the bombarding energy calculated with the parameterisation of J. Cugnon et al. [14].

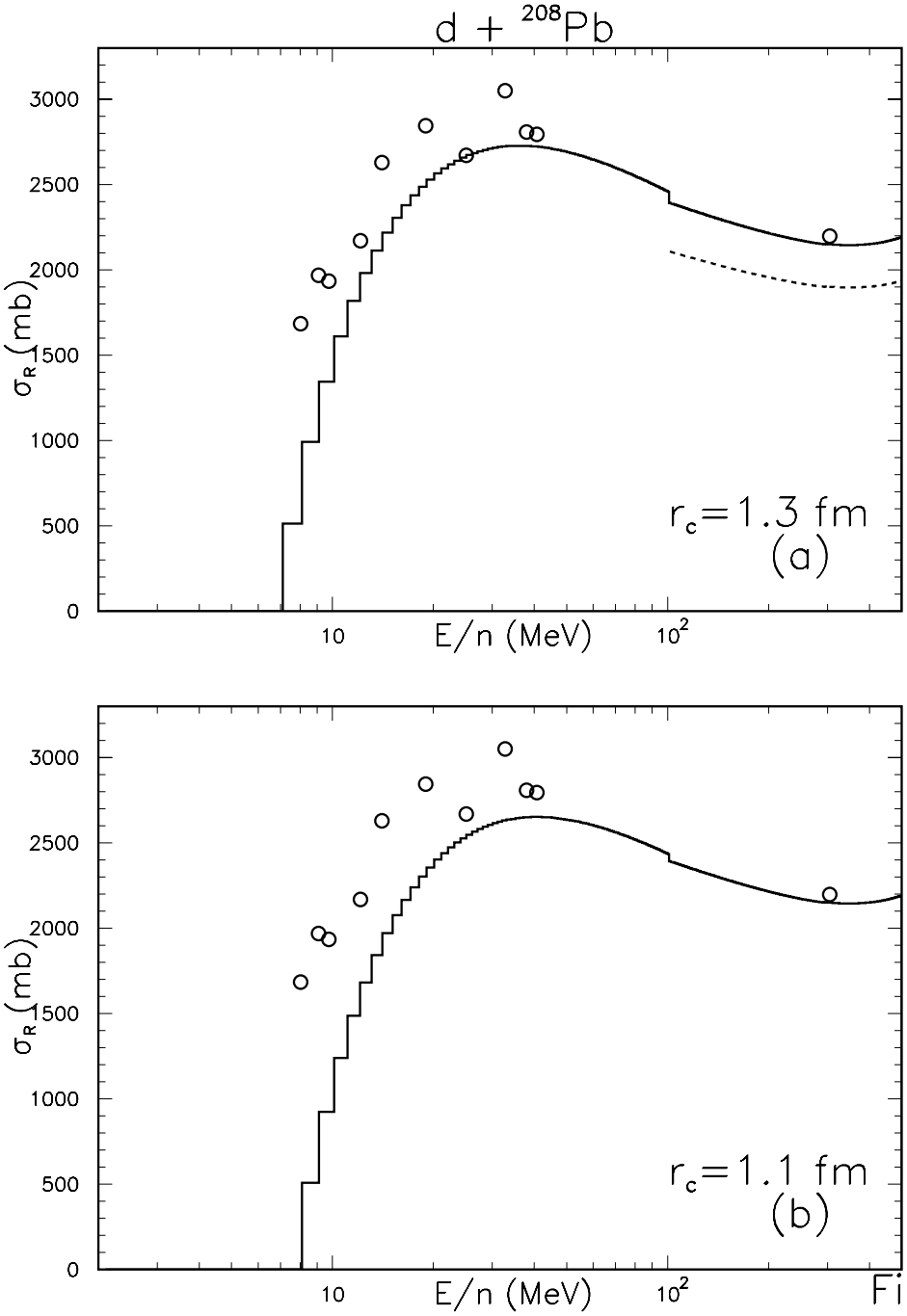

Fig.1

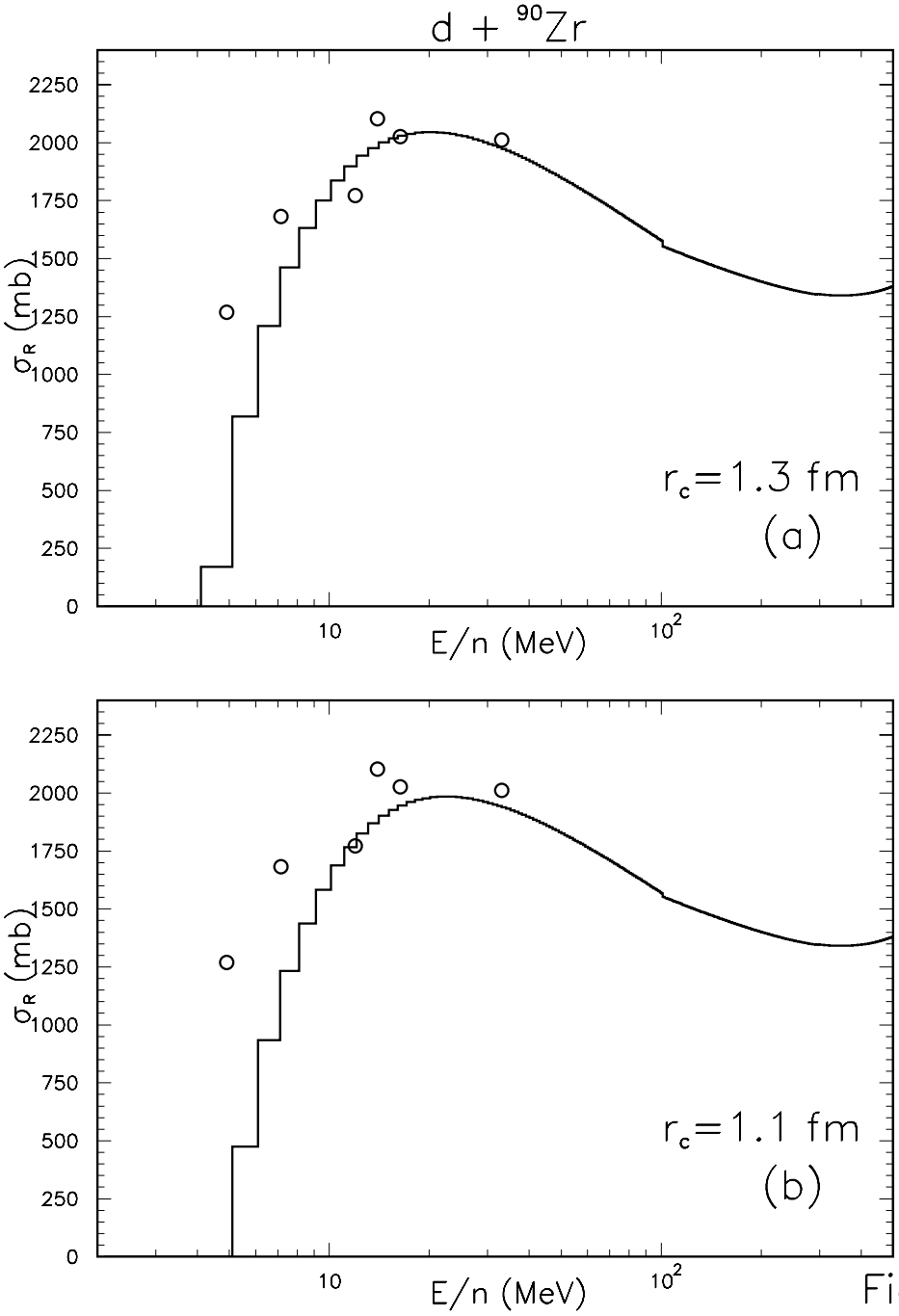

Fig.2

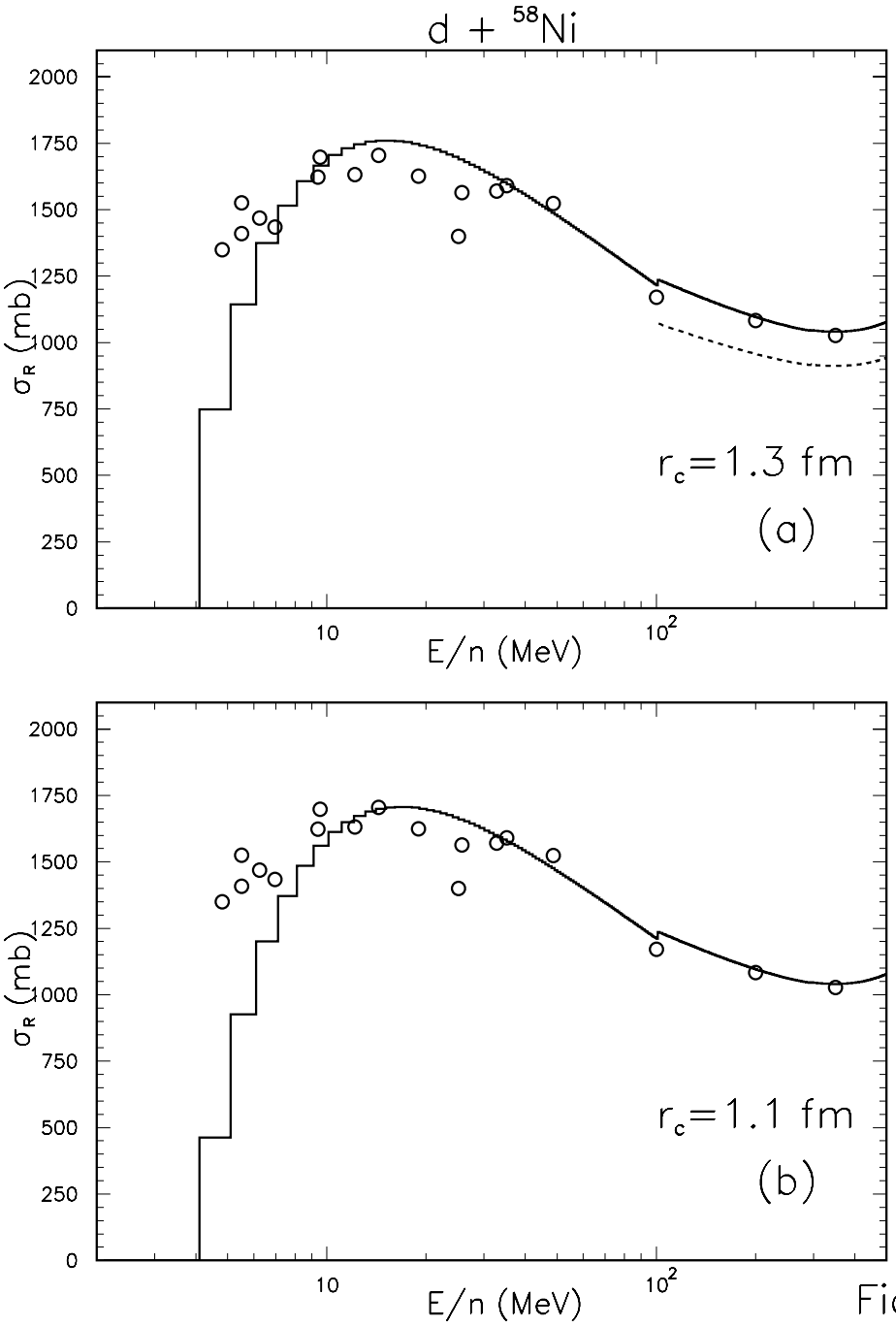

Fig.3

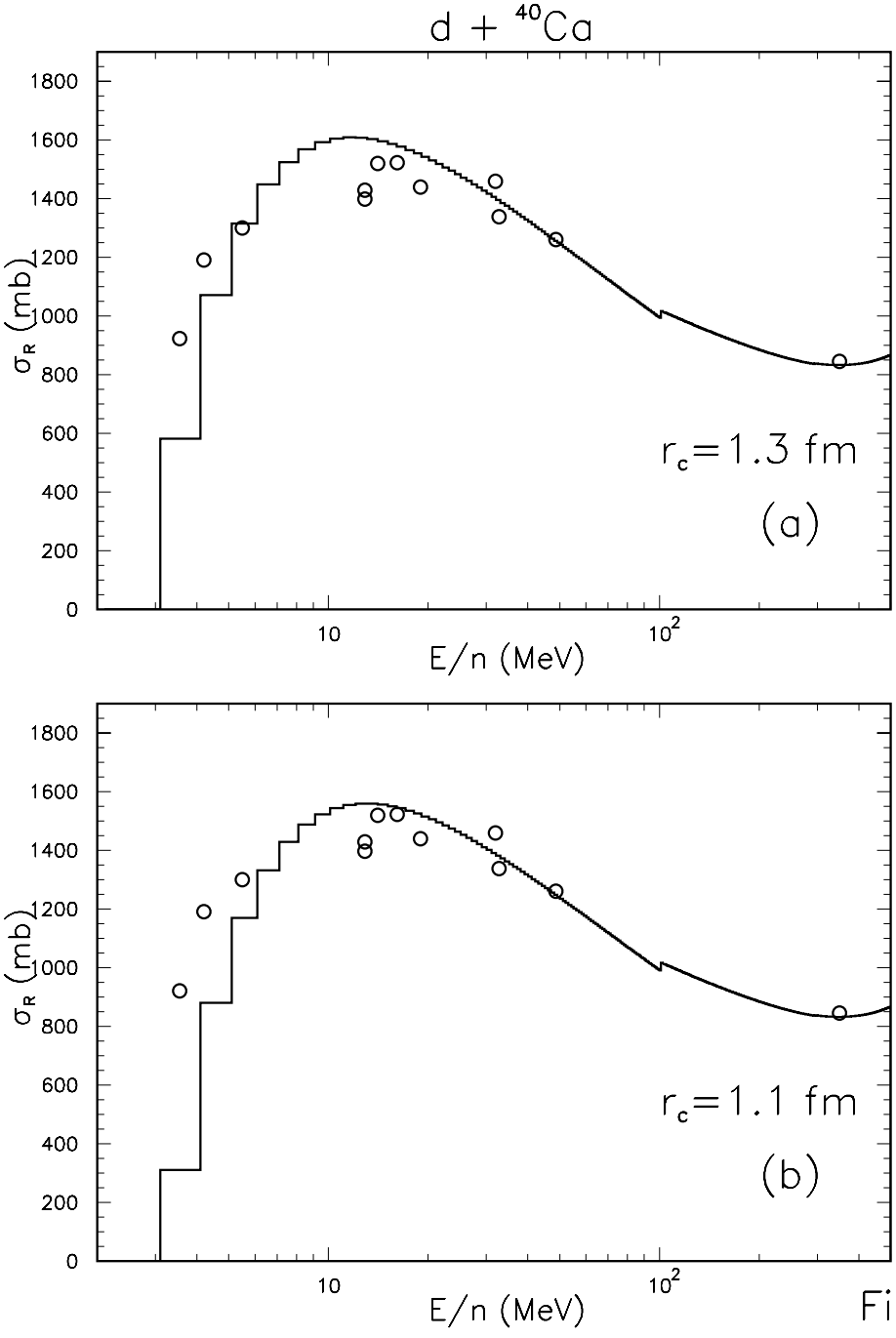

Fig.4

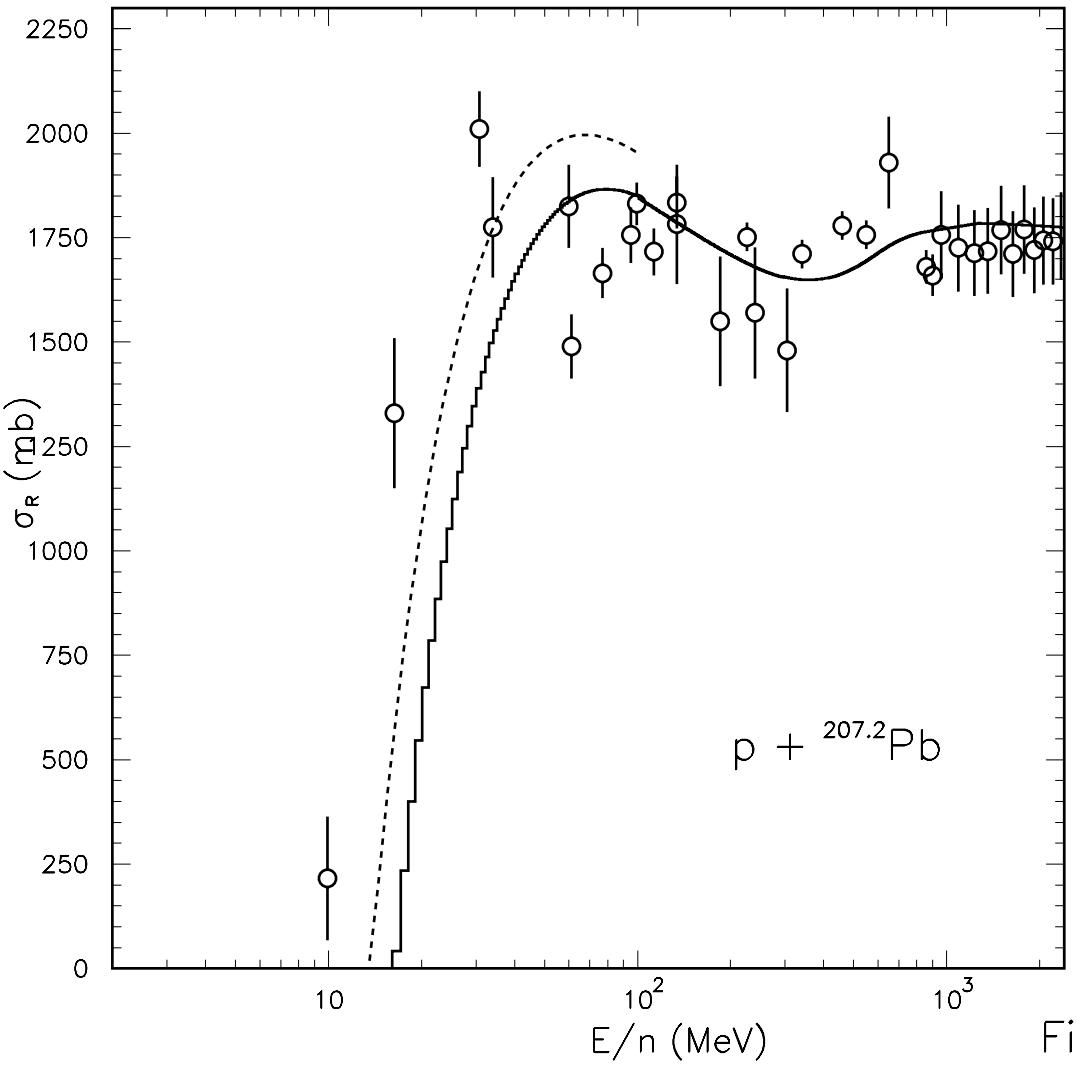
2250
2000
1750
1500
1250
1000
750
500
250
0
σ_R (mb)
10
10^2
10^3
E/n (MeV)
p + $^{207.2}$Pb

Fig.5

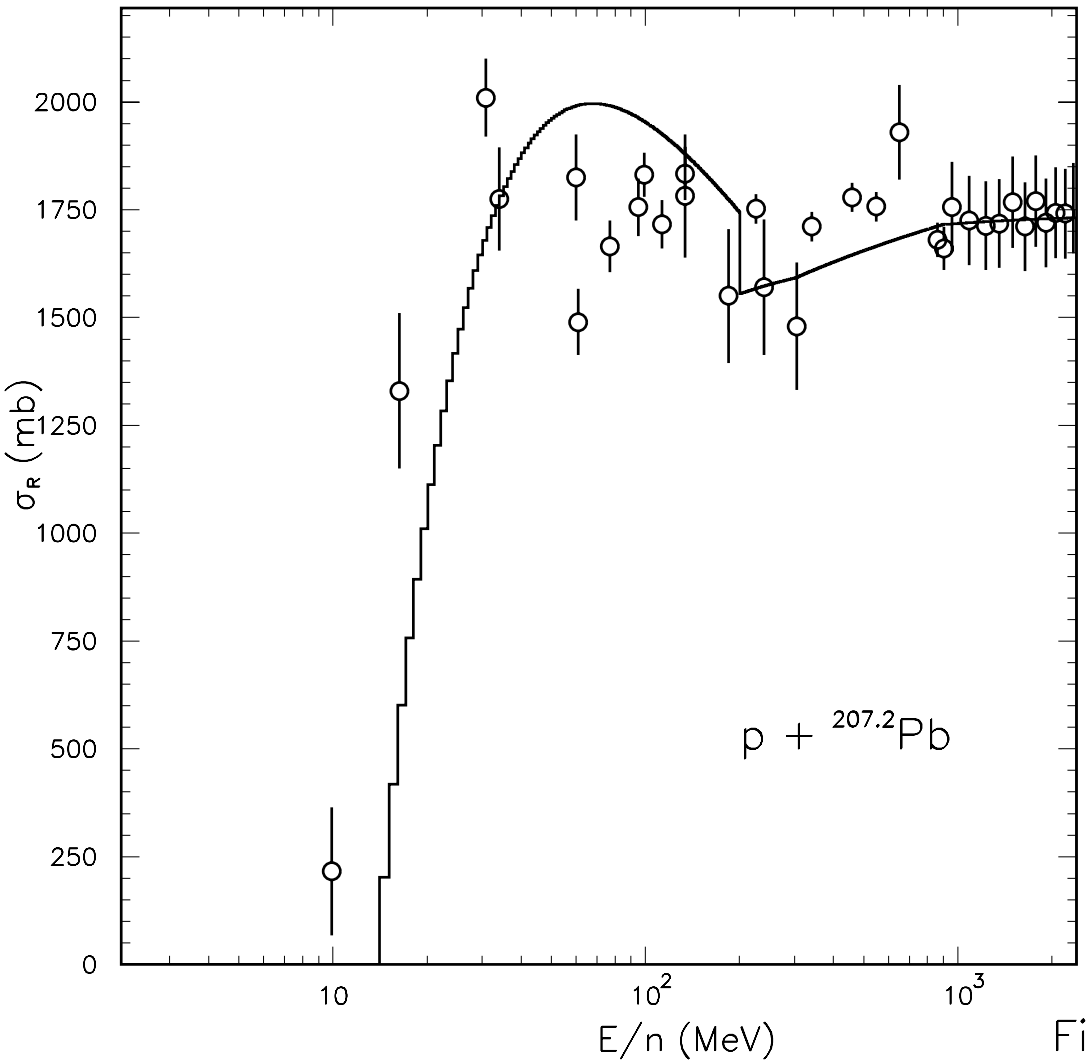
2000
1750
1500
1250
1000
750
500
250
0
σ_R (mb)
10
10^2
10^3
E/n (MeV)
p + $^{207.2}$Pb

Fig.6

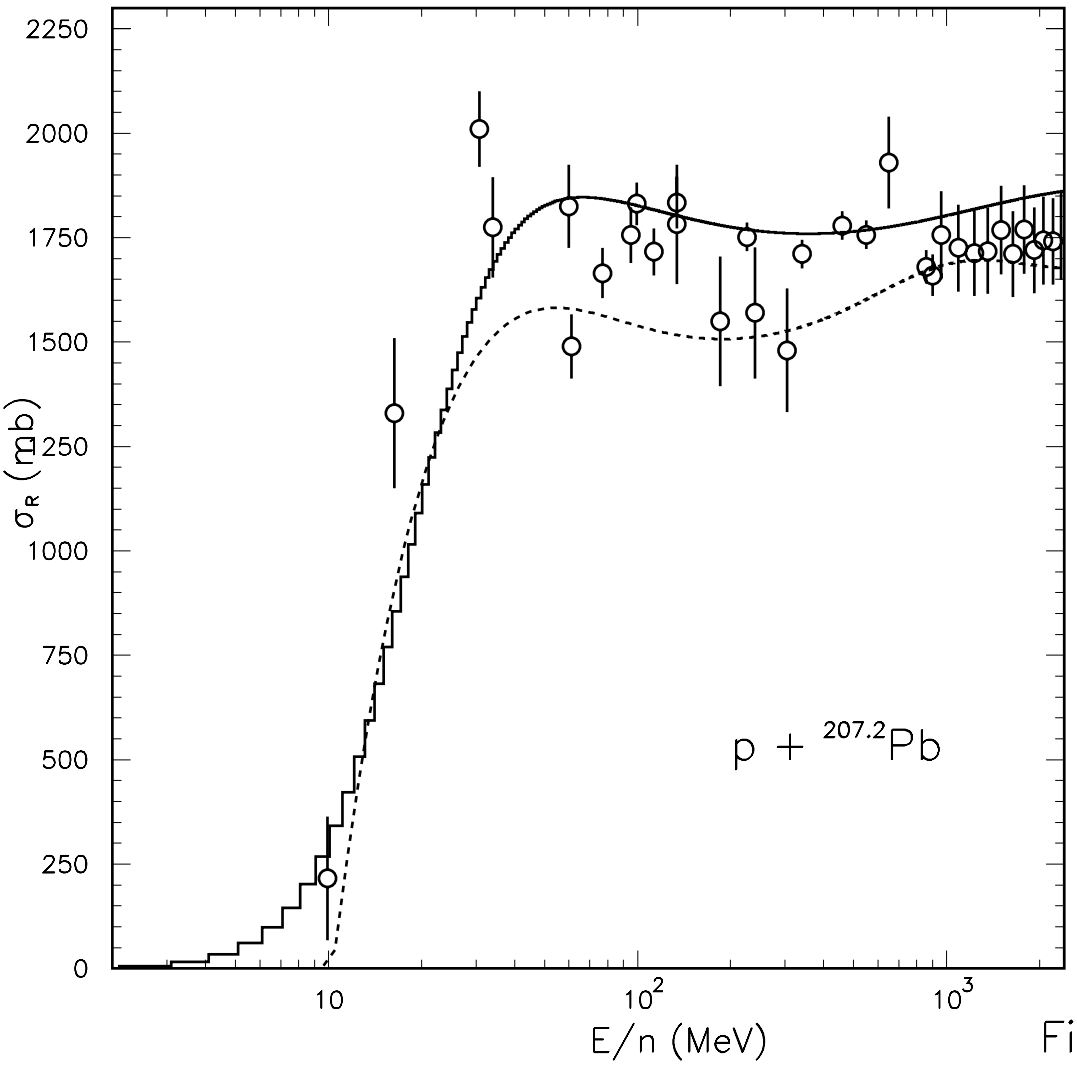
2250
2000
1750
1500
1250
1000
750
500
250
0
σ_R (mb)
10
10^2
10^3
E/n (MeV)
p + $^{207.2}$Pb

Fig.7

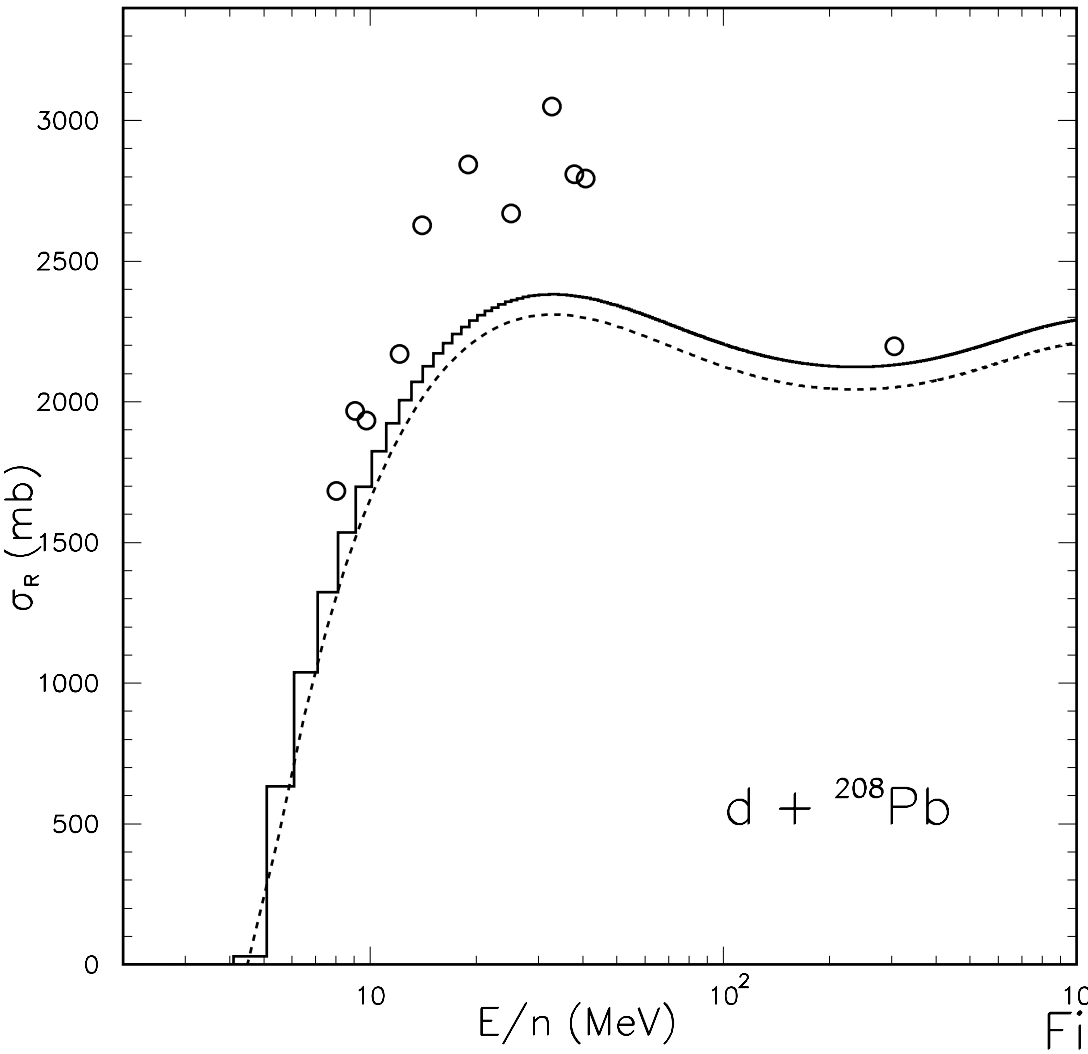
3000
2500
2000
1500
1000
500
0
σ_R (mb)
10
10^2
10^3
E/n (MeV)
d + ^{208}Pb

Fig.8

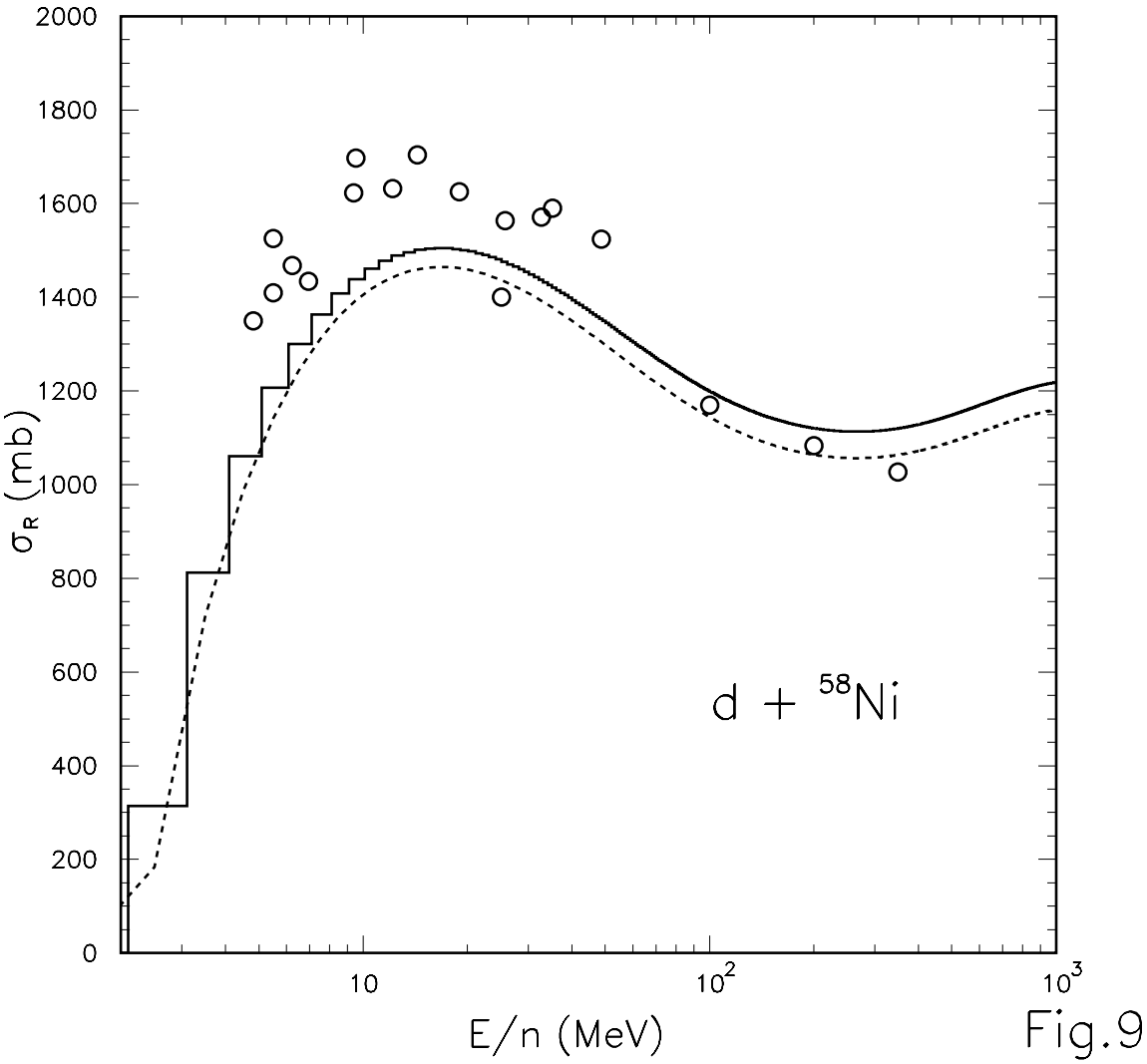
2000
1800
1600
1400
1200
1000
800
600
400
200
0
σ_R (mb)
10
10^2
10^3
E/n (MeV)
d + ^{58}Ni

Fig.9

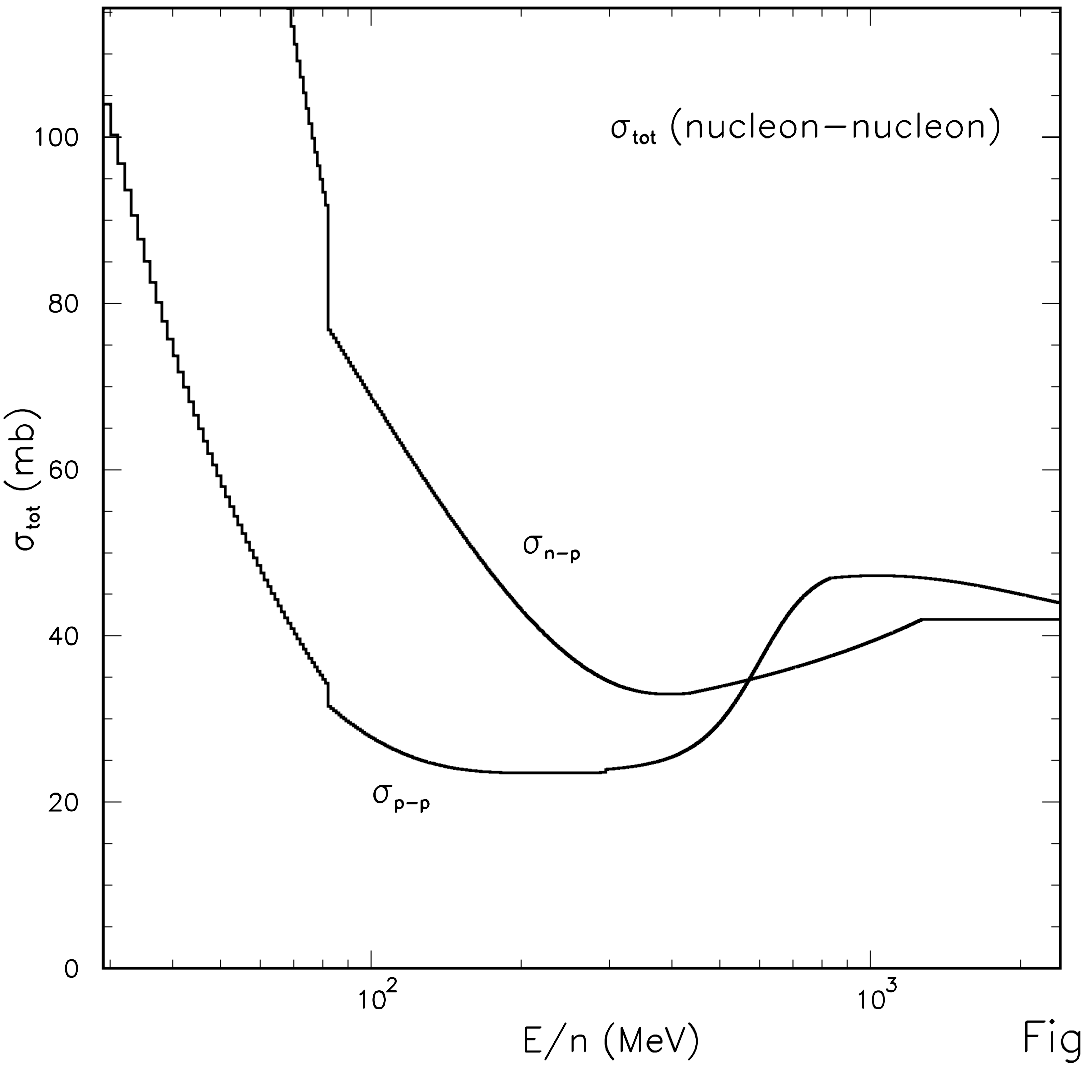
σtot (nucleon−nucleon)
σn−p
σp−p
σtot (mb)
E/n (MeV)
0
20
40
60
80
100
10^2
10^3

Fig.10